SUPPLEMENTAL INFORMATION

Profiling the Essential Nature of Lipid Metabolism in Asexual Blood Stages and Gametocytes of *Plasmodium falciparum* Malaria Parasites

Sonia Gulati, Eric H. Ekland, Kelly V. Ruggles, Robin B. Chan, Bamini Jayabalasingham, Bowen Zhou, Pierre-Yves Mantel, Marcus C. S. Lee, Natasha Spottiswoode, Olivia Coburn-Flynn, Daisy Hjelmqvist, Tilla S. Worgall, Matthias Marti, Gilbert Di Paolo and David A. Fidock

Figure S1

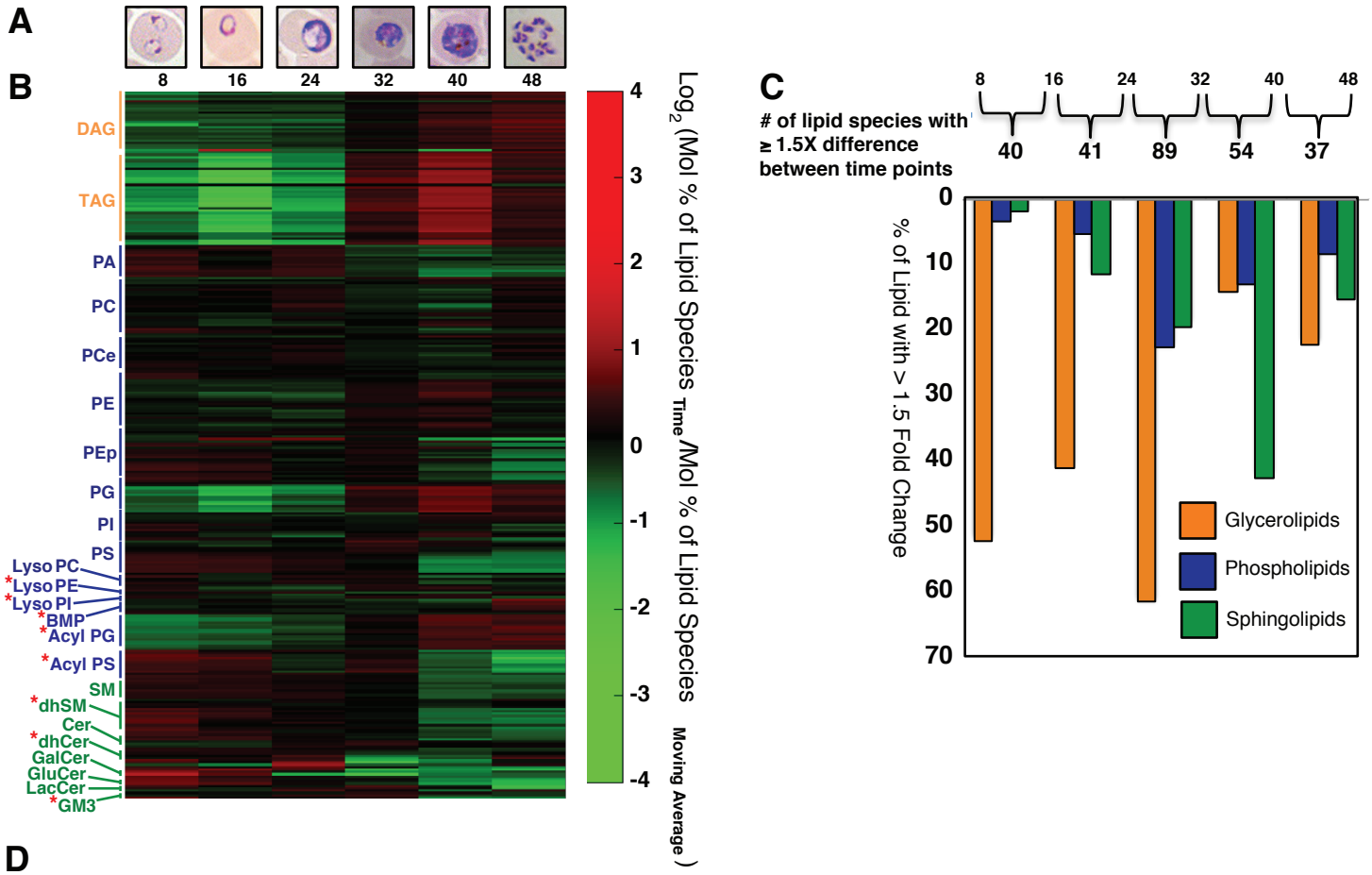
A
8
16
24
32
40
48
B
DAG
TAG
PA
PC
PCe
PE
PEp
PG
PI
PS
Lyso PC
*Lyso PE
*Lyso PI
*BMP
*Acyl PG
*Acyl PS
SM
*dhSM
Cer
*dhCer
GalCer
GluCer
LacCer
*GM3
4
3
2
1
0
-1
-2
-3
-4
Log2 (Mol % of Lipid Species Time /Mol % of Lipid Species Moving Average)
C
# of lipid species with ≥ 1.5X difference between time points
8
16
24
32
40
48
40
41
89
54
37
% of Lipid with > 1.5 Fold Change
0
10
20
30
40
50
60
70
Glycerolipids
Phospholipids
Sphingolipids
D
Magnet-purified infected RBCs
Uninfected RBCs
Mol% of total lipids measured
35%
30%
25%
20%
15%
10%
5%
0%
PC
PE
PS
PI
PA
PG
Acyl PS
Acyl PG
Lyso PI
Lyso PE
Lyso PC
BMP
SM
dhSM
Cer
LacCer
GM3
Lipid species

Figure S2

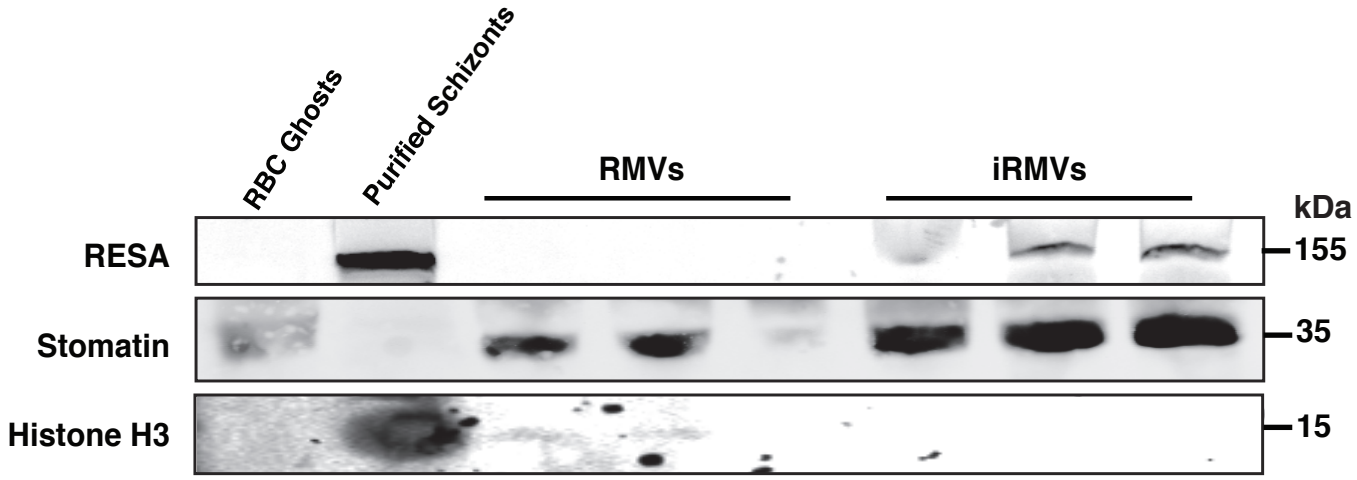
RBC Ghosts
Purified Schizonts
RMVs
iRMVs
kDa
RESA
155
Stomatin
35
Histone H3
15

Figure S3

A

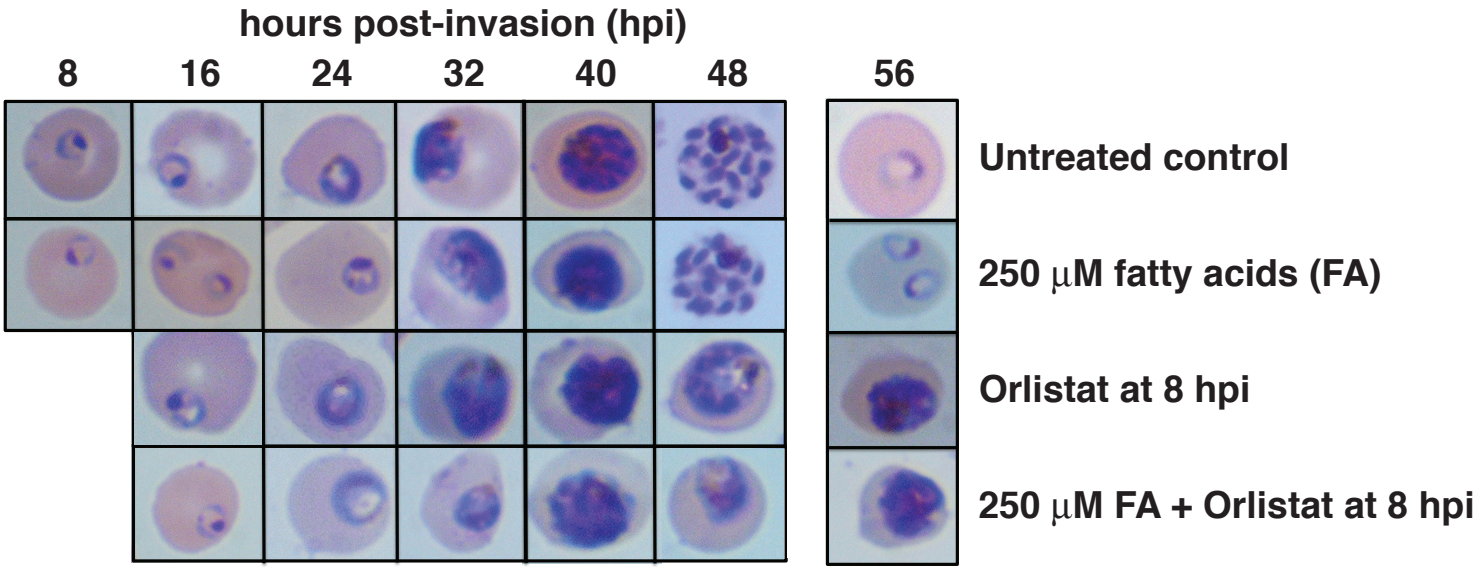

B **LC-MS analysis of lipid species in drug-treated parasites**

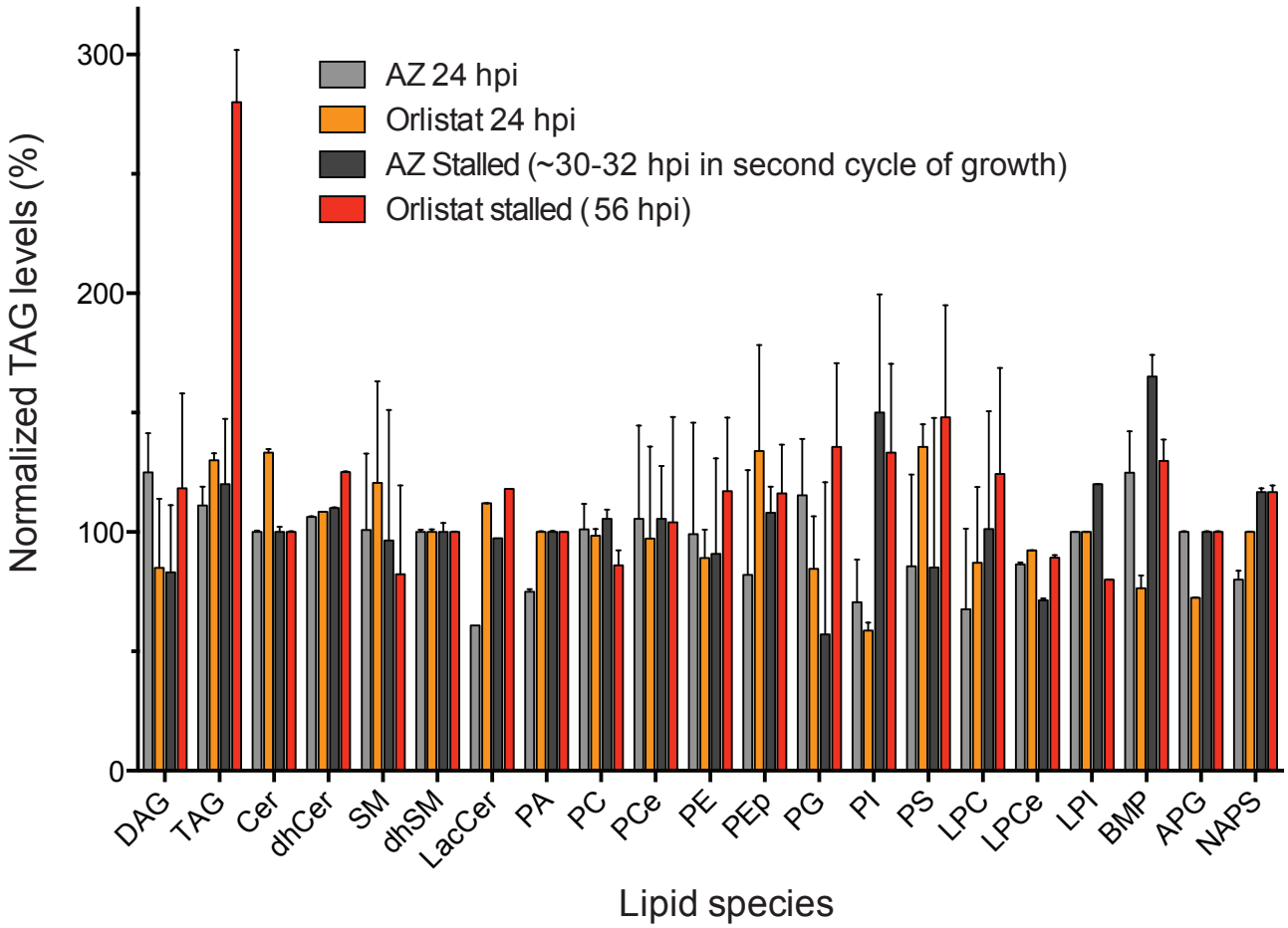

Figure S4

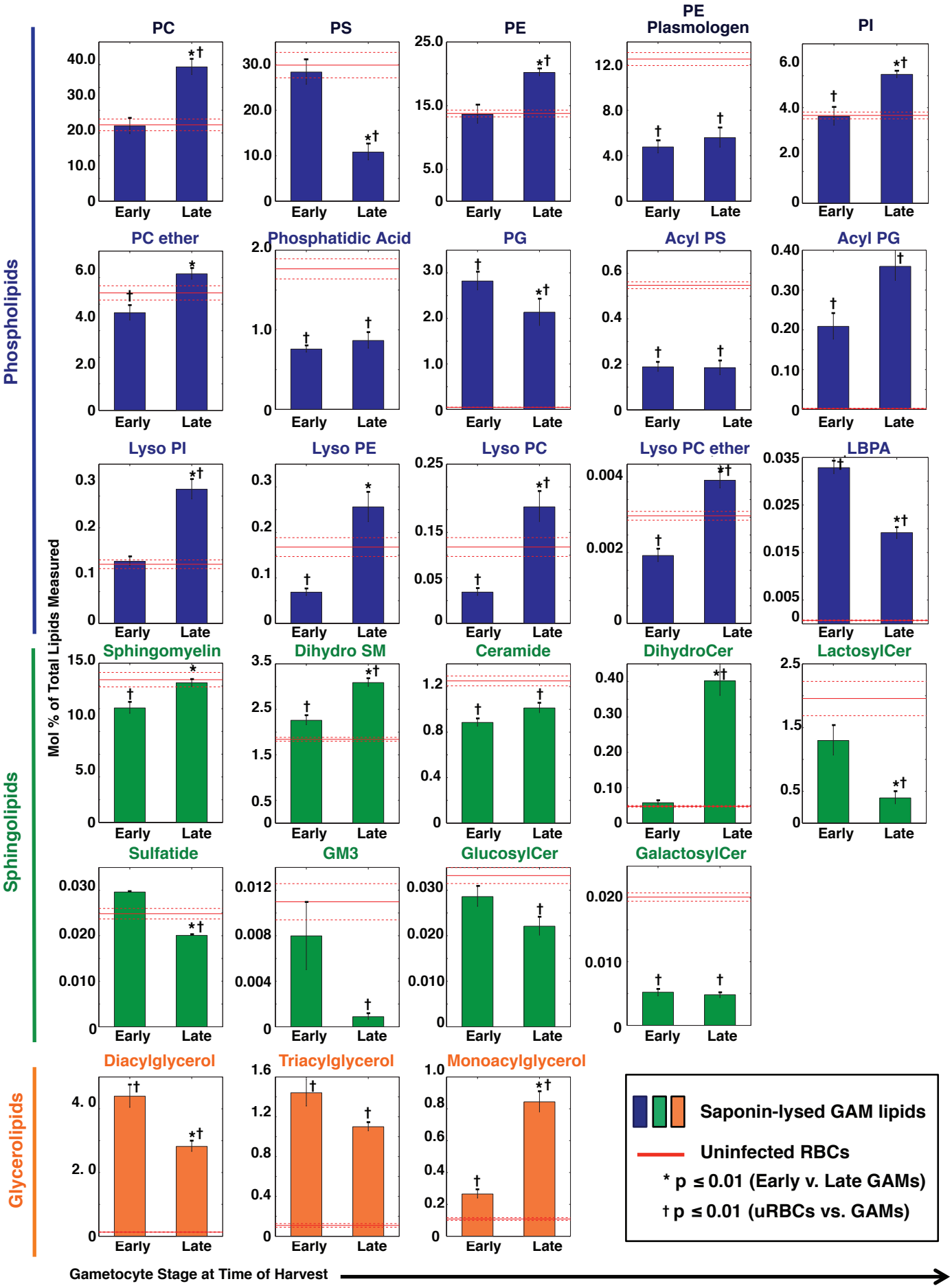
Phospholipids
Sphingolipids
Glycerolipids
Mol % of Total Lipids Measured
PC
PS
PE
PE Plasmologen
PI
PC ether
Phosphatidic Acid
PG
Acyl PS
Acyl PG
Lyso PI
Lyso PE
Lyso PC
Lyso PC ether
LBPA
Sphingomyelin
Dihydro SM
Ceramide
DihydroCer
LactosylCer
Sulfatide
GM3
GlucosylCer
GalactosylCer
Diacylglycerol
Triacylglycerol
Monoacylglycerol
Early
Late
Saponin-lysed GAM lipids
Uninfected RBCs
* p ≤ 0.01 (Early v. Late GAMs)
† p ≤ 0.01 (uRBCs vs. GAMs)
Gametocyte Stage at Time of Harvest

SUPPLEMENTAL FIGURE LEGENDS

Figure S1, related to Figure 1. Lipidomic profiling of ABS parasites. (A, B) Highly synchronized Dd2 cultures were harvested every 8 hr post merozoite invasion and 304 individual lipid species were quantified via LC-MS/MS. The mole percent of each lipid species was averaged across time to obtain the moving average value. The $\log_2$ ratio was then calculated for each lipid species at each time point and normalized to the moving average. Each row in the heatmap represents an individual lipid species. Phospholipid, sphingolipid, and glycerolipid species are shown in blue, green, and orange respectively. Lipid species that have not been previously identified in *P. falciparum* are indicated with an asterisk. Shown below the heatmap is a summary of the total number of lipid species that exhibit at least a 1.5 fold difference between adjacent time points. As an example, 40 lipid species were found to differ by at least 1.5–fold between the 8 and 16 hr time points. (C) Percentage of each lipid class that showed a ≥ 1.5 fold difference between adjacent time points (e.g. between 8 and 16 hpi, 53% of the all glycerolipids showed a greater than 1.5 fold difference). (D) Lipid profile of magnet-purified *P. falciparum* trophozoites (32–40 hours post-invasion). These data were obtained in triplicate and lipids were extracted and processed as per the method for saponin-lysed parasites. Results show a clear concordance across almost all lipid species with data shown for trophozoite stages in Figure 1, which did not use magnet enrichment as it profiled across all stages of the intra-erythrocytic developmental cycle. Blue boxes indicate lipid species that were increased in both types of analyses in the parasite samples compared to uninfected RBCs. The orange boxes indicate lipid species that were decreased in both types of analyses. These results also closely reproduced the saponin-lysed parasite data (Figure 1 and Table S1) in terms of the relative abundances and Mol% values of the major species. Discordant results were observed only for the minor species Acyl PS, Lyso PE and Lyso PC, for which the low Mol% values (<0.2% of total for each) might have reduced the accuracy. BMP, bis(monoacylglyceryl)phosphate; Cer, ceramide; DAG, diacylglycerol; dhCer, dihydroceramide; dhSM, dihydrosphingomyelin; GalCer, galactosylceramide; GluCer, glucosylceramide; GM3, monosialodihexosylganglioside; LacCer, lactosylceramide; PA, phosphatidic acid; PC, phosphatidylcholine; PCe, PC ether; PE, phosphatidylethanolamine; Pep, PE plasmologen; PG,

phosphatidylglycerol; PI, phosphatidylinositol; PS, phosphatidylserine; SM, sphingomyelin; TAG, triacylglycerol; uRBCs, uninfected RBCs.

Figure S2, related to Figure 2. SDS-PAGE (polyacrylamide gel electrophoresis) and immunoblot analysis of red blood cell microvesicle (RMV) fractions. Samples were collected and purified as described in the Supplemental Experimental Procedures section above. For SDS-PAGE pellets were washed 3 times in 1×PBS and resuspended in reducing SDS sample buffer (Invitrogen). Proteins were separated on 4–12% Bis-Tris gels (Invitrogen). For Western blots, proteins were transferred onto 0.45 μm PVDF membranes. Samples were probed with the following antibodies: anti-Histone H3 (1:10000 Abcam) a marker for merozoites and schizonts; anti-Stomatin (1:2000, clone M-14; Santa Cruz Biotechnologies) a marker for RMVs; anti-RESA (1:500, (Brown et al., 1985)), a marker for iRMVs (Mantel et al., 2013).

Figure S3, related to Figure 3. Evidence that Orlistat inhibition of P. falciparum ABS growth is not rescued by exogenous fatty acid, and operates via inhibition of triacylglycerol degradation. (A) Exogenous fatty acids do not rescue the Orlistat maturation block. Dd2 parasites were highly synchronized by sorbitol treatment for two successive growth cycles, and then diluted to 3% parasitemia in 2% hematocrit in a 24 well plate. Parasites were cultured in control media containing 0.5% Albumax or in the same media supplemented with oleic acid (18:1) and palmitic acid (16:0) at 250 μM each. Wells were treated with or without 6 μM Orlistat (8× IC_{50}) at 8, 16, 24, 32, 40, or 48 hr. ABS development was then assayed by Giemsa stain every 8 hr up to 56 hr. Appropriate media and Orlistat treatments were replaced every 8 hr. Representative images for each condition at each time point are shown. The addition of exogenous oleic acid (18:1) and palmitic acid (16:0) showed no phenotypic rescue of Orlistat-treated parasites. We posit that the addition of exogenous fatty acids could not substitute for the rapid and localized intracellular release of fatty acids that occurs via lipase-mediated hydrolysis and that was blocked by Orlistat action (Kurat et al., 2006). (B) Orlistat inhibits triacylglycerol degradation in *P. falciparum* mature ABS parasites. Highly synchronized parasites (6–8

hpi) were exposed to Orlistat or the unrelated delayed death drug and apicoplast inhibitor azithromycin (AZ), and samples harvested at 24 hpi and later when parasite development had stalled. Stalled parasites were harvested at 56 hpi for Orlistat, corresponding to a time when schizonts had not matured and were unable to egress (**Figure 3B**). AZ-treated were harvested after 72 hr of exposure, corresponding to ~30–32 hpi in the second cycle when AZ action has blocked further growth as a result of its delayed death action (AZ-treated parasites die during the next generation of intracellular growth; Sidhu et al, 2007). Control parasites were treated with DMSO vehicle and harvested at the same time points as drug-treated samples. Lipids were extracted, subjected to mass spectrometry, and levels in drug-treated parasites calculated as a percentage of levels measured in DMSO-treated control parasites. Experiments were performed on two separate occasions in duplicate, and are presented as means±SEM. Data show a substantial increase specifically in TAG levels in the Orlistat-treated parasites harvested as mature schizonts that had developmentally stalled. These data independently agree with results from thin layer chromatography (**Figure 3C**). APG=acyl phosphatidylglycerol; BMP=bis(monoacylglyceryl)phosphate; Cer=Ceramide, DAG=diacylglycerol, dhCer=dihydroceramide; dhSM=dihydrosphingomyelin; LacCer=lactosylceramide; LPC=lactosyl-phosphatidylcholine; LPCe=LPC ether; LPI=lactosyl phosphatidylinositol; NAPS=acyl phosphatidylserine; PI=phosphatidylinositol; PA=phosphatidic acid; PC=phosphatidylcholine; PCe=PC ether; PE=phosphatidylethanolamine; PEp=PE plasmologen; PG=phosphatidylglycerol; PI=phosphatidylinositol; PS=phosphatidylserine; SM=sphingomyelin; TAG=triacylglycerol.

Figure S4, related to Figure 5. Composition of lipid species in *P. falciparum* early and late stage gametocytes and host red blood cells. Twenty-seven lipid species from saponin lysed early- or late-stage gametocytes (GAMs) and uninfected RBCs were harvested and quantified via LC-MS/MS. Gametocyte and uninfected red blood cell (uRBC) samples were collected and harvested at two time points, 3-5 days (corresponding to Stages I–II) and 10-12 days (corresponding to Stages IV–V) post-induction of gametocytes. Data are shown as means±SEM (n=3 independent experiments performed in triplicate). There was no significant difference in the relative abundance of RBC lipids

harvested at the two time points and therefore RBCs are depicted as a single red line. SEM is shown as dashed red lines. Student's t-tests were used to identify significant differences between either uninfected RBCs and gametocytes (**†=** p≤0.01) or early and late gametocytes (*p≤0.01). Cer=Ceramide, GM3= monosialodihexosylganglioside, LBPA=lysobisphospha-tidic acid, PC=phosphatidylcholine, PE= phosphatidylethanolamine, PG=phosphatidylglycerol, PI=phosphatidylinositol, PS=phosphatidylserine, SM, sphingomyelin.

Table S1, related to Figure 1. Analysis of individual lipid species in *P. falciparum* asexual blood stage parasites and uninfected red blood cells.

Table S2, related to Figure 3. Antimalarial IC_{50} values of compounds active against lipid metabolic pathways.

Table S3, related to Figure 5. Lipidomic analysis of individual lipid species in *P. falciparum* gametocytes and uninfected red blood cells.

Table S2, related to Figure 3. Antimalarial IC_{50} values of compounds active against lipid metabolic pathways.

Compound	Mode of Action	Reference	Lipid	ABS IC_{50} (μM)
CAY10499	Hormone Sensitive Lipase	(Manna et al., 2013)	GL	1.2 ± 0.5**
Quercetin	Pancreatic Lipase	(Gatto et al., 2002)	GL	5.0 ± 1.6
Orlistat	Pancreatic Lipase	(Guerciolini, 1997)	GL	0.9 ± 0.1
URB602	MAG Lipase	(King et al., 2007)	GL	> 25
T863	Acyl CoA:Diacylglycerol O-acyltransferase 1	(Cao et al., 2011)	GL	> 10
Dioctanoylglycol	Diacylglycerol Kinase	(Ganong et al., 1986)	PL	> 50
R 59-022	Diacylglycerol Kinase	(Ohtsuka et al., 1990)	PL	6.3 ± 0.9
Pioglitazone	Acyl CoA Synthetase	(Kim et al., 2001)	PL, GL	> 12.5
Rosiglitazone	Acyl CoA Synthetase	(Kim et al., 2001)	PL, GL	> 35
RHC 80267	Diacylglycerol Lipase	(Ghisdal et al., 2005)	PL	> 25
CI-976	Lysophospholipid acyltransferase	(Brown et al., 2008)	PL	> 25
MJ33	Phospholipase A2	(Fisher et al., 1992)	PL	> 10
Ezetimibe	Niemann Pick C-1 Like 1	(Garcia-Calvo et al., 2005)	Sterol	12.5 ± 2.4
N-Butyldeoxynojirimycin	Glucosylceramide Synthase	(Platt et al., 1994)	SL	> 25
DL-*threo*-1-Phenyl-2-palmitoylamino-3-morpholino-1-propanol	Glucosylceramide Synthase	(Stefanic et al., 2010)	SL	0.9 ± 0.3
GT11	Dihydroceramide Desaturase	(Bedia et al., 2005)	SL	> 8
N-(4-hydroxyphenyl) retinamide	Unknown (ceramide accumulation)	(Delgado et al., 2006)	SL	3.5 ± 0.8
MSDH-C	Dihydroceramide synthase	(Betz et al., 2003)	SL	> 10
GW4869	Neutral Sphingomyelinase	(Trajkovic et al., 2008)	SL	0.006 ± 0.0003
Epoxyquinone	Neutral Sphingomyelinase	(Cutler et al., 2014)	SL	1.9 ± 0.4
Spiroepoxide	Neutral Sphingomyelinase	(Delgado et al., 2006)	SL	> 10
Sphingolactone-24	Neutral Sphingomyelinase	(Lin et al., 2011)	SL	> 20
3-O-Methylsphingomyelin	Neutral Sphingomyelinase	(Delgado et al., 2006)	SL	6.2 ± 1.2
N,N-Dimethylsphingosine (NNDMS)	Sphingosine Kinase	(McDonald et al., 2010)	SL	2.2 ± 0.6
Ceranib	Ceramidase	(Draper et al., 2011)	SL	14.6 ± 2.3
NVP-231	Ceramide Kinase	(Pastukhov et al., 2014)	SL	> 10
Tricyclodecan-9-yl-xanthogenate	Sphingomyelin Synthase	(Adibhatla et al., 2012)	SL	> 25

Compounds were tested against *Plasmodium falciparum* asexual blood stage N54 parasites in 72-hr assays over 10 two–fold concentrations, as described in the Supplemental Experimental Procedures. Mean±SEM IC_{50} values were determined from four independent experiments performed in duplicate. GL, glycerolipid (i.e. neutral lipid), SL, sphingolipid, PL, phospholipid. **CAY10499 exhibited a 5-fold shift in IC_{50} values between 48 hr and 96 hr, suggesting a delayed death phenotype.

SUPPLEMENTAL EXPERIMENTAL PROCEDURES

Plasmodium falciparum Asexual Blood Stage Cultures and Synchronization and Saponin Lysis

Dd2 parasites were maintained in human red blood cells (RBCs), cultured in RPMI 1640 complete medium containing 0.5% Albumax as described (Fidock et al., 1998) and expanded to 8-10% parasitemia prior to harvesting. NF54 cultures were maintained in RPMI 1640 culture medium supplemented with 10% human serum. NF54 and Dd2 cultures were synchronized with 5% D-sorbitol (w/v) treatment for 10 minutes at 37ºC for two or more successive growth cycles. Culture flasks were incubated at 37°C with gentle shaking overnight to promote optimal re-invasion. To prepare ABS parasite samples for lipid analysis, we typically began with 75 mL cultures at 8–10% parasitemia and 4–6% hematocrit (corresponding to $3.2–6.0\times10^7$ infected RBC). Cultures were centrifuged and the medium removed. Cell pellets were then resuspended in 40 mL total (~10–fold excess) of 1×PBS buffer containing 0.1% saponin and incubated for 10–15 minutes. Cells were then recentrifuged to pellet the parasites, colored brown because of the internal hemozoin. A white layer of RBC membrane could be seen that typically sediments above the parasite pellets; this layer was carefully pipetted away while removing the supernatant. Pellets at this point were typically ~0.5–1.0 mL. These were washed an additional 3-4 times, or until the supernatant became clear, with 15 mL 1×PBS buffer to remove any residual hemoglobin and further remove RBC membrane, thus ensuring a low residual RBC component in the final saponin-lysed parasite fraction.

Lipid analysis was also performed with magnet-purified trophozoite-infected RBCs. Comparisons with the saponin-lysed parasite samples showed highly concordant results, with both preparations showing the same major lipid species and very similar Mol% values of total lipid measured (**Figure S1D**). Both methods also yielded similar amounts of individual lipid species in parasite preparations vs. uninfected RBCs. Magnet enrichment, however, cannot be used to purify young ring-stage parasites. Furthermore, the purification procedure required 1–2 hours to complete, during which time the parasites were under undue stress due to being in an oxygenated environment at ambient temperature, and added a new variable into the time course. Saponin lysis was therefore chosen as

the reference method that could be used equally across all stages of intra-erythrocytic parasite development. Of note, saponin lysis is an established method to lyse the RBC membrane and leave the parasite membrane intact for further lipidomic, metabolomic or proteomic analysis (Botte et al., 2013; Vo Duy et al., 2012; Wu et al., 2006).

Gametocyte Commitment and Harvesting

To produce *P. falciparum* gametocytes, 300 mL cultures of asexual blood stage (ABS) NF54 parasites were first synchronized with 5% D-sorbitol (w/v) treatment for 10 minutes at 37ºC for two or more successive growth cycles. 2-3% synchronous trophozoites were then incubated overnight to obtain about 8-10% ring-stage parasites. Cultures were stressed by replacing 50% of the spent medium with fresh medium (referred to in the main text as “50% conditioned media”). This is a standard protocol to induce gametocytes (Buchholz et al., 2011; Fivelman et al., 2007). On the next day (designated as day −1), when parasites reached trophozoite stage, the medium was changed and the culture was diluted 2–fold. On the following day, Day 0, 50 mM N-acetyl glucosamine (NAG) was added to ring-stage parasites. NAG treatment was maintained for the next two to three cycles of reinvasion to eliminate all asexual forms from the culture. Immature gametocytes (Stages I–II) and mature gametocytes (Stage IV–V) were harvested on days 2–4 and 10–12 respectively. Harvested cultures were lysed with 0.01% saponin, washed 3-4 times with 1×PBS and frozen. Gametocytemias at time of harvest were 3–4% and was determined by flow cytometry (Eckland et al., 2011) and confirmed by Giemsa stain. In brief, 100 μL of the gametocyte culture was added to a 96-well flat bottom plate. The culture was stained with 1.6 μM Mito Tracker Deep Red (Molecular Probes, Eugene, OR, USA) and 2× SYBR Green (Invitrogen) diluted in culture medium.

Analysis of Lipids Using High Performance Liquid Chromatography-Mass Spectrometry

Lipids were extracted from uninfected RBCs, RBC microvesicles, Dd2 parasites, and gametocytes, using methods described in (Hara and Radin, 1978). Briefly, 2 mL of isopropanol: hexane (1: 2) and 2 ml of KCl (2 M): MeOH (4: 1) were added to cell pellets. Samples were mixed and centrifuged at

4,000 RPM for five minutes. The organic (top) layer was removed and the pellet was re-extracted with 2 ml of isopropanol:hexane (1: 2). The organic phase was dried with nitrogen gas and resuspended in 500 μL hexane (Tinkelenberg et al., 2000). The samples were dried down again with nitrogen gas and resuspended in 300 μL chloroform: methanol (2: 1). These organic solvents serve as fixatives that ablate any protein activity in the cell, lipases included (Lux et al., 2014). As an extra precaution, 1M KCl was included during the extraction procedure to block the binding of some acidic lipids to denatured proteins (Hajra, 1974).

Lipid extracts were analyzed using a 6490 Triple Quadrupole LC/MS system and were spiked with appropriate internal standards (Agilent Technologies, Santa Clara, CA). Glycerophospholipids and sphingolipids were separated with normal-phase HPLC, essentially as described (Chan et al., 2012). An Agilent Zorbax Rx-Sil column (inner diameter 2.1 x 100 mm) was used under the following conditions: mobile phase A (chloroform: methanol: 1 M ammonium hydroxide, 89.9:10:0.1, v/v) and mobile phase B (chloroform: methanol: water: ammonium hydroxide, 55:39.9:5:0.1, v/v); 95% A for 2 min, linear gradient to 30% A over 18 min and held for 3 min, and linear gradient to 95% A over 2 min and held for 6 min. Sterols and glycerolipids were separated with reverse-phase HPLC using an isocratic mobile phase (Chan et al., 2012) with an Agilent Zorbax Eclipse XDB-C18 column (4.6 x 100 mm). Quantification of lipid species was accomplished using multiple reaction monitoring (MRM) transitions that were developed in earlier studies (Chan et al., 2012; Guan et al., 2007; Hsu et al., 2004) in conjunction with referencing of appropriate internal standards: PA 14:0/14:0, PC 14:0/14:0, PE 14:0/14:0, PG 15:0/15:0, PI 16:0/16:0, PS 14:0/14:0, BMP 14:0/14:0, APG 14:0/14:0, LPC 17:0, LPE 14:0, LPI 13:0, Cer d18:1/17:0, SM d18:1/12:0, dhSM d18:0/12:0, GalCer d18:1/12:0, GluCer d18:1/12:0, LacCer d18:1/12:0, MG 17:0, 4ME 16:0 diether DG, D_5-TG 16:0/18:0/16:0 (Avanti Polar Lipids, Alabaster, AL).

Individual lipid species for ABS parasites and gametocytes are provided in Tables S1 and S3 respectively. Of note, for DAG and TAG lipid species we presented the parent (or composite) fatty

acid ion and the most abundant daughter fatty acid ion. This method will not cover the entire DAG and TAG combinations but proved necessary, as DAG and TAG do not produce specific diagnostic daughter ions, unlike phospholipids. For example, for the lipid species DAG 36:0/18:0, 36:0 represents the parent ion, which is the composite of both fatty acid chains present, and 18:0 represents the most abundant daughter or individual fatty acid chain found in that molecule. In the case of TAG, with the lipid species TAG 60:9/22:6 for example, 60:9 represents the parent ion, which is the composite of all three fatty acid chains present, and 22:6 represents one possible daughter ion or individual fatty acid chain found in the parent ion. Because of the extensive number of possible fatty acid permutations for TAGs, we typically documented the parent/daughter pair that represented the greatest number of combinations of a specific TAG molecule. In both cases, the daughter ion was determined by the fragmentation of the parent ion and the m/z value corresponding to the respective daughter ion.

Measurement of S1P Levels in NNDMS-Treated *P. falciparum* ABS Parasites and Gametocytes. Synchronized *P. falciparum* ABS parasites, tested at the early ring stage (4–8 hours post invasion), were exposed to the Sphingosine 1 kinase inhibitor NNDMS (N,N-Dimethylsphingosine, 5 $\times IC_{50}$, equal to 11 μM), or malaria culture medium as a control, for 12 hr. Parasites were then harvested, the lipids extracted, and samples subjected to mass spectrometry with internal standards, as detailed below. Separately, early to mid stage gametocytes (stages II–IV) were also generated *in vitro* and the lipids extracted and quantified by mass spectrometry. Experiments were performed on two separate occasions in triplicate.

S1P levels were measured as reported (Bui et al., 2012). Briefly, samples were extracted in 2 mL 96-well plates overnight in a 1:30 v/v solution of dichloromethanol: methanol 1:1, diethylamide 10%, and vortexed at room temperature using C12 sphingomyelin (Avanti Polar Lipids) as internal standard. After centrifuging the plate for 10 min, 100 μL of supernatant was transferred into a clean plate, and a 3 μL aliquot was chromatographed on an Agilent 1200 HPLC using a Poroshell 120 EC-C18 column.

S1P peaks were detected by Agilent 6430 triple quadrupole-tandem mass spectrometry, with external standards run in parallel to provide a quantitation from 14-250 pmol. Measurements were performed in triplicates and normalized to protein. Mean±SEM S1P levels in untreated ABS parasites, NNDMS-treated ABS parasites, and untreated gametocytes were 9,911±3,295, 4,471±737 and 2,128±468 picomoles of S1P / mg of total parasite protein. Statistical significance was determined using Student *t* tests that compared untreated ABS parasites vs. either NNDMS-treated ABS ring-stage parasites or gametocytes. This showed significantly lower S1P levels in both NNDMS-treated ABS parasites and untreated gametocytes as compared with untreated ABS parasites, with a *p* value < 0.05

Data Analysis

Outliers (±2 standard deviations from the mean) within each time point and lipid species for each sample time (uninfected RBC, infected RBC, parasite, early/late gametocytes and supernatant) were filtered prior to lipidomic analyses. Data were represented using the following equations (Guan et al., 2013).

Mol% of the lipid species *n* as a function of total lipids $= \frac{lipid_n\ (mol)}{\sum membrane\ lipids\ (mol)}$ (Equation 1)

Mol% of lipid class *N* as a function of total lipids $= \frac{\sum lipid\ species\ in\ classN\ (mol)}{\sum membrane\ lipids\ (mol)}$ (Equation 2)

Mol% moving average of lipid species *n* $=$ average mol% of lipid species n across time (Equation 3)

Relative deviation from moving average $= LOG2\left(\frac{mol\%\ at\ time\ t\ (Eq.1)}{mol\%\ of\ moving\ average\ (Eq.3)}\right)$ (Equation 4)

Comparison of the means of lipid species and classes were performed between times (8, 16, 24, 32, 40 and 48 hr), as well as between uninfected RBCs (controls) and saponin-lysed parasites. Additionally, means of lipid species and classes were compared between early and late gametocytes. Statistical tests were performed using a one-way analysis of variants (ANOVA) and Student *t* tests in MATLAB R2012b and a *p*-value less than 0.05 was considered to be statistically significant. Additionally the mol% for chain length and saturation categories were calculated within each lipid

class, and statistical comparisons were made to identify changing length/saturation across time and between RBC, saponin-lysed parasites, and gametocytes.

Determination of Stage Specific Inhibition by Drugs

A highly synchronized ring-stage *P. falciparum* Dd2 culture was diluted to 3% parasitemia with a 2% hematocrit in a 24 well plate. Orlistat or GW4869 were added at 6 μM and 1 μM concentrations respectively, at different time intervals for 48 hr after merozoite invasion. Culture media and drug was changed every 8 hr. Parasite development was monitored every 8 hr by Giemsa staining.

Lipid labeling and Thin Layer Chromatography

Five ml cultures of synchronized Dd2 parasites (at 4–5% parasitemia) were cultured in complete media. At 6 hr post-invasion (hpi), the media was supplemented with 1 μCi/mL [9,10-^{3}H]Oleic acid (Perkin Elmer Life Sciences). In addition, we added 6 μM Orlistat (8×IC_{50}) or 136 nM Azithromycin (8×IC_{50}) or DMSO vehicle. IC_{50} values represent the drug concentration that produced half-maximal inhibition of parasite growth in 72 hr assays (as described below) (new). The culture media was changed every 8 hr. Parasites were harvested at 24 hpi for all conditions. Orlistat-treated and untreated cultures were also harvested at 56 hpi. Azithromycin treated-parasites and untreated parasites were harvested at 72 hpi. Harvested parasites were washed and lysed in 0.1% Saponin. Parasite pellets were washed 3–4 times with 1×PBS and stored at -80°C. Lipids were extracted as described above. The organic phases were dried down and resolved by thin layer chromatography in petroleum ether/diethyl ether/acetic acid (84:15:1). Lipids were detected using iodine staining and quantified via scintillation counting, as described in (Freeman and West, 1966; Wilcox et al., 2002). Separately, extracted lipids were quantified by mass spectrometry (see **Figure S4**).

Physical Disruption/Merozoite Release Assay

Synchronized trophozoite cultures (starting 36-40 hpi) were treated with either DMSO, 1 μM E-64 (a protease inhibitor that blocks merozoite release from schizonts and parasite egress from infected RBCs; (Blackman, 2008)), 125 nM KAI407 (a PI4(K) inhibitor that blocks parasite membrane ingression and merozoite egress (McNamara et al., 2013; Zou et al., 2014), or 6 μM Orlistat ($8\times IC_{50}$). At 56 hpi, parasites were collected and passed through a 1.2 μm filter as previously described (Boyle et al., 2010). The cultures were incubated for an additional 72 hr and parasitemias were determined by flow cytometry.

Imaging of PfATP4-GFP Labeled Plasma Membrane in Orlistat-Treated Parasites

Sorbitol-synchronized parasites expressing the plasma membrane protein PfATP4, fused to GFP (Rottmann et al., 2010), were treated at 24 hpi with either 6 μM Orlistat or DMSO (control), and incubated for an additional 28 hr. Cells were imaged using a Nikon TiE PFS inverted microscope equipped with a CoolSNAP HQ2 monochrome camera.

ABS and Gametocyte *In Vitro D*rug Susceptibility Assays

In vitro IC_{50} values were determined by incubating ABS parasites or gametocytes (for 48, 72 or 96 hr, as designated in the text) with compounds diluted 2–fold across 10 concentrations. Methylene Blue was added as a positive control (Adjalley et al., 2011), with a maximum concentration of 250 nM. Assays were performed in duplicate on three independent occasions. Final parasitemias in drug-treated or control untreated wells were determined using flow cytometry. For this, cells were stained with 1.6 μM Mito Tracker Deep Red and 2×SYBR Green (Invitrogen) in culture media, and analyzed on an Accuri C6 flow cytometer (Ekland et al., 2011). *In vitro* IC_{50} values were calculated by non-linear regression analysis and Student *t*-tests were employed for statistical analysis.

Preparation of RMVs and Other Cellular Samples

RMVs (microvesicles derived from RBCs) were isolated by a combination of sequential rounds of centrifugation at increasing speed, high molecular weight cut-off filters and a one-step sucrose gradient. Purity of resulting samples was controlled by Western blot analysis of different fractions. Samples were probed with anti-Histone H3 (a marker for merozoites and schizonts), anti-Stomatin (a marker for the RMV fraction), and anti-RESA (a marker for iRMVs, i.e. RMVs from cultures of infected RBCs), as previously described (Mantel et al., 2013).

Staining Neutral Lipids with BODIPY 493/503

Synchronized trophozoite cultures (32 hpi) and gametocytes were stained with 2 μg/ml BODIPY 495/503 and 2 μg/ml Hoechst 33342 in RPMI 1640 incomplete medium (lacking Albumax). Cells were incubated for ten minutes at 37ºC and imaged immediately.

SUPPLEMENTARY REFERENCES (INCLUDING FROM TABLE S2)

Adibhatla, R.M., Hatcher, J.F., and Gusain, A. (2012). Tricyclodecan-9-yl-xanthogenate (D609) mechanism of actions: a mini-review of literature. Neurochem Res *37*, 671-679.

Bedia, C., Triola, G., Casas, J., Llebaria, A., and Fabrias, G. (2005). Analogs of the dihydroceramide desaturase inhibitor GT11 modified at the amide function: synthesis and biological activities. Org Biomol Chem *3*, 3707-3712.

Betz, R., Sandhoff, K., Fischer, K.D., and van Echten-Deckert, G. (2003). Detection and identification of Vav1 protein in primary cultured murine cerebellar neurons and in neuroblastoma cells (SH-SY5Y and Neuro-2a). Neurosci Lett *339*, 37-40.

Blackman, M.J. (2008). Malarial proteases and host cell egress: an 'emerging' cascade. Cell Microbiol *10*, 1925-1934.

Brown, G.V., Culvenor, J.G., Crewther, P.E., Bianco, A.E., Coppel, R.L., Saint, R.B., Stahl, H.D., Kemp, D.J., and Anders, R.F. (1985). Localization of the ring-infected erythrocyte surface antigen (RESA) of *Plasmodium falciparum* in merozoites and ring-infected erythrocytes. J Exp Med *162*, 774-779.

Brown, W.J., Plutner, H., Drecktrah, D., Judson, B.L., and Balch, W.E. (2008). The lysophospholipid acyltransferase antagonist CI-976 inhibits a late step in COPII vesicle budding. Traffic *9*, 786-797.

Buchholz, K., Burke, T.A., Williamson, K.C., Wiegand, R.C., Wirth, D.F., and Marti, M. (2011). A high-throughput screen targeting malaria transmission stages opens new avenues for drug development. J Infect Dis *203*, 1445-1453.

Bui, H.H., Leohr, J.K., and Kuo, M.S. (2012). Analysis of sphingolipids in extracted human plasma using liquid chromatography electrospray ionization tandem mass spectrometry. Anal Biochem *423*, 187-194.

Cao, J., Zhou, Y., Peng, H., Huang, X., Stahler, S., Suri, V., Qadri, A., Gareski, T., Jones, J., Hahm, S.*, et al.* (2011). Targeting Acyl-CoA:diacylglycerol acyltransferase 1 (DGAT1) with small molecule inhibitors for the treatment of metabolic diseases. J Biol Chem *286*, 41838-41851.

Chan, R.B., Oliveira, T.G., Cortes, E.P., Honig, L.S., Duff, K.E., Small, S.A., Wenk, M.R., Shui, G., and Di Paolo, G. (2012). Comparative lipidomic analysis of mouse and human brain with Alzheimer disease. J Biol Chem *287*, 2678-2688.

Cutler, R.G., Thompson, K.W. Cutler, R.G., Thompson, K.W., Camandola, S., Mack, K.T., and Mattson, M.P. (2014). Sphingolipid metabolism regulates development and lifespan in *Caenorhabditis elegans*. Mech Ageing Dev *143-144*, 9-18.

Delgado, A., Casas, J., Llebaria, A., Abad, J.L., and Fabrias, G. (2006). Inhibitors of sphingolipid metabolism enzymes. Biochim Biophys Acta *1758*, 1957-1977.

Draper, J.M., Xia, Z., Smith, R.A., Zhuang, Y., Wang, W., and Smith, C.D. (2011). Discovery and evaluation of inhibitors of human ceramidase. Mol Cancer Ther *10*, 2052-2061.

Ekland, E.H., Schneider, J., and Fidock, D.A. (2011). Identifying apicoplast-targeting antimalarials using high-throughput compatible approaches. FASEB J *25*, 3583-3593.

Fidock, D.A., Nomura, T., and Wellems, T.E. (1998). Cycloguanil and its parent compound proguanil demonstrate distinct activities against *Plasmodium falciparum* malaria parasites transformed with human dihydrofolate reductase. Mol Pharmacol *54*, 1140-1147.

Fisher, A.B., Dodia, C., Chander, A., and Jain, M. (1992). A competitive inhibitor of phospholipase A2 decreases surfactant phosphatidylcholine degradation by the rat lung. Biochem J *288*, 407-411.

Freeman, C.P., and West, D. (1966). Complete separation of lipid classes on a single thin-layer plate. J Lipid Res *7*, 324-327.

Ganong, B.R., Loomis, C.R., Hannun, Y.A., and Bell, R.M. (1986). Specificity and mechanism of protein kinase C activation by sn-1,2-diacylglycerols. Proc Natl Acad Sci USA *83*, 1184-1188.

Garcia-Calvo, M., Lisnock, J., Bull, H.G., Hawes, B.E., Burnett, D.A., Braun, M.P., Crona, J.H., Davis, H.R., Jr., Dean, D.C., Detmers, P.A.*, et al.* (2005). The target of ezetimibe is Niemann-Pick C1-Like 1 (NPC1L1). Proc Natl Acad Sci USA *102*, 8132-8137.

Gatto, M.T., Falcocchio, S., Grippa, E., Mazzanti, G., Battinelli, L., Nicolosi, G., Lambusta, D., and Saso, L. (2002). Antimicrobial and anti-lipase activity of quercetin and its C2-C16 3-O-acyl-esters. Bioorg Med Chem *10*, 269-272.

Ghisdal, P., Vandenberg, G., Hamaide, M.C., Wibo, M., and Morel, N. (2005). The diacylglycerol lipase inhibitor RHC-80267 potentiates the relaxation to acetylcholine in rat mesenteric artery by anti-cholinesterase action. Eur J Pharmacol *517*, 97-102.

Guan, X.L., Cestra, G., Shui, G., Kuhrs, A., Schittenhelm, R.B., Hafen, E., van der Goot, F.G., Robinett, C.C., Gatti, M., Gonzalez-Gaitan, M.*, et al.* (2013). Biochemical membrane lipidomics during *Drosophila* development. Dev Cell *24*, 98-111.

Guerciolini, R. (1997). Mode of action of orlistat. Int J Obes Relat Metab Disord *21 Suppl 3*, S12-23.

Hajra, A.K. (1974). On extraction of acyl and alkyl dihydroxyacetone phosphate from incubation mixtures. Lipids *9*, 502-505.

Hsu, F.F., Turk, J., Shi, Y., and Groisman, E.A. (2004). Characterization of acylphosphatidylglycerols from *Salmonella typhimurium* by tandem mass spectrometry with electrospray ionization. J Am Soc Mass Spectrom *15*, 1-11.

Kim, J.H., Lewin, T.M., and Coleman, R.A. (2001). Expression and characterization of recombinant rat Acyl-CoA synthetases 1, 4, and 5. Selective inhibition by triacsin C and thiazolidinediones. J Biol Chem *276*, 24667-24673.

King, A.R., Duranti, A., Tontini, A., Rivara, S., Rosengarth, A., Clapper, J.R., Astarita, G., Geaga, J.A., Luecke, H., Mor, M.*, et al.* (2007). URB602 inhibits monoacylglycerol lipase and selectively blocks 2-arachidonoylglycerol degradation in intact brain slices. Chem Biol *14*, 1357-1365.

Lin, W.C., Lin, C.F., Chen, C.L., Chen, C.W., and Lin, Y.S. (2011). Inhibition of neutrophil apoptosis via sphingolipid signaling in acute lung injury. J Pharmacol Exp Ther *339*, 45-53.

Lux, G., Mansfeld, J., and Ulbrich-Hofmann, R. (2014). Phospholipase A(2)-catalyzed acylation of lysophospholipids analyzed by experimental design. Enzyme Microb Technol *64-65*, 60-66.

Manna, P.R., Cohen-Tannoudji, J., Counis, R., Garner, C.W., Huhtaniemi, I., Kraemer, F.B., and Stocco, D.M. (2013). Mechanisms of action of hormone-sensitive lipase in mouse Leydig cells: its role in the regulation of the steroidogenic acute regulatory protein. J Biol Chem *288*, 8505-8518.

McDonald, R.A., Pyne, S., Pyne, N.J., Grant, A., Wainwright, C.L., and Wadsworth, R.M. (2010). The sphingosine kinase inhibitor N,N-dimethylsphingosine inhibits neointimal hyperplasia. Br J Pharmacol *159*, 543-553.

Ohtsuka, T., Hiura, M., Yoshida, K., Okamura, N., and Ishibashi, S. (1990). A diacylglycerol kinase inhibitor, R 59 022, potentiates superoxide anion production and 46-kDa protein phosphorylation in guinea pig polymorphonuclear leukocytes. J Biol Chem *265*, 15418-15423.

Pastukhov, O., Schwalm, S., Zangemeister-Wittke, U., Fabbro, D., Bornancin, F., Japtok, L., Kleuser, B., Pfeilschifter, J., and Huwiler, A. (2014). The ceramide kinase inhibitor NVP-231 inhibits breast and lung cancer cell proliferation by inducing M phase arrest and subsequent cell death. Br J Pharmacol *171*, 5829-5844.

Platt, F.M., Neises, G.R., Dwek, R.A., and Butters, T.D. (1994). N-butyldeoxynojirimycin is a novel inhibitor of glycolipid biosynthesis. J Biol Chem *269*, 8362-8365.

Stefanic, S., Spycher, C., Morf, L., Fabrias, G., Casas, J., Schraner, E., Wild, P., Hehl, A.B., and Sonda, S. (2010). Glucosylceramide synthesis inhibition affects cell cycle progression, membrane trafficking, and stage differentiation in *Giardia lamblia*. J Lipid Res *51*, 2527-2545.

Trajkovic, K., Hsu, C., Chiantia, S., Rajendran, L., Wenzel, D., Wieland, F., Schwille, P., Brugger, B., and Simons, M. (2008). Ceramide triggers budding of exosome vesicles into multivesicular endosomes. Science *319*, 1244-1247.

Vo Duy, S., Besteiro, S., Berry, L., Perigaud, C., Bressolle, F., Vial, H.J., and Lefebvre-Tournier, I. (2012). A quantitative liquid chromatography tandem mass spectrometry method for metabolomic analysis of *Plasmodium falciparum* lipid related metabolites. Anal Chim Acta *739*, 47-55.

Wilcox, L.J., Balderes, D.A., Wharton, B., Tinkelenberg, A.H., Rao, G., and Sturley, S.L. (2002). Transcriptional profiling identifies two members of the ATP-binding cassette transporter superfamily required for sterol uptake in yeast. J Biol Chem *277*, 32466-32472.

Wu, Y., and Craig, A. (2006). Comparative proteomic analysis of metabolically labelled proteins from *Plasmodium falciparum* isolates with different adhesion properties. Malar J *5*, 67.

Zou, B., Nagle, A., Chatterjee, A.K., Leong, S.Y., Tan, L.J., Sim, W.L., Mishra, P., Guntapalli, P., Tully, D.C., Lakshminarayana, S.B.*, et al.* (2014). Lead optimization of imidazopyrazines: a new class of antimalarial with activity on *Plasmodium* liver stages. ACS Med Chem Lett *5*, 947-950.